Molecular BioSystems

Dynamic Article Links

Cite this: *Mol. BioSyst.*, 2011, **7**, 2637–2650

www.rsc.org/molecularbiosystems

PAPER

Proteomic responses in *Arabidopsis thaliana* seedlings treated with ethylene†

Ruiqiang Chen,[a] Brad M. Binder,[b] Wesley M. Garrett,[c] Mark L. Tucker,[d] Caren Chang‡*[a] and Bret Cooper‡*[d]

Received 26th April 2011, Accepted 2nd June 2011
DOI: 10.1039/c1mb05159h

Ethylene (ET) is a volatile hormone that modulates fruit ripening, plant growth, development and stress responses. Key components of the ET-signaling pathway identified by genetic dissection in *Arabidopsis thaliana* include five ET receptors, the negative regulator CTR1 and the positive regulator EIN2, all of which localize to the endoplasmic reticulum. Mechanisms of signaling among these proteins are still unresolved and targets of ET responses are not fully known. So, we used mass spectrometry to identify proteins in microsomal membrane preparations from etiolated *A. thaliana* seedlings maintained in ambient air or treated with ET for 3 h. We compared 3814 proteins from ET-exposed seedlings and controls and identified 304 proteins with significant accumulation changes. The proteins with increased accumulation were involved in ET biosynthesis, cell morphogenesis, oxidative stress and vesicle secretion while those with decreased accumulation were ribosomal proteins and proteins positively regulated by brassinosteroid, another hormone involved in cell elongation. Several proteins, including EIN2, appeared to be differentially phosphorylated upon ET treatment, which suggests that the activity or stability of these proteins may be controlled by phosphorylation. TUA3, a component of microtubules that contributes to cellular morphological change, exhibited both increased accumulation and differential phosphorylation upon ET treatment. To verify the role of TUA3 in the ET response, *tua3* mutants were evaluated. Mutant seedlings had altered ET-associated growth movements. The data indicate that ET perception leads to rapid proteomic change and that these changes are an important part of signaling and development. The data serve as a foundation for exploring ET signaling through systems biology.

Introduction

Ethylene (ET) is a gaseous molecule that has numerous effects on plant growth and displays complex interactions with other endogenous plant hormones, growth regulators and environmental factors to provide fine-tuning of development and adaptation.[1] Components of the ET-perception signal transduction pathway have been identified, mostly through forward-genetics in *Arabidopsis thaliana*. ET is perceived by a family of membrane-bound, homo- and heterodimeric receptors residing at the endoplasmic reticulum (ER) and possibly the Golgi apparatus.[2–7] One receptor displays His auto-kinase activity while the others exhibit Ser/Thr kinase activity, or both, *in vitro*.[8,9] The roles of their kinase activities and their *in vivo* substrates are unknown. The receptors repress ET responses in the absence of ET by activating CTR1[10] although there may also be an alternate ET-response pathway that bypasses CTR1.[11,12] CTR1 is a negative regulator of ET response, resides at the ER due to physical association with the receptors and has sequence similarity to Raf-like protein kinases.[13,14] The next known genetic downstream component, EIN2 (ETHYLENE INSENSITIVE 2), is a critical, positive regulator of ET-signal transduction, but its biochemical function is unknown.[15] EIN2 also localizes to the ER where it possibly interacts with the ETR1 ethylene receptor.[16] Genetically downstream of EIN2 are transcription factors (TF) EIN3 and EIL1, which activate the expression of another TF, ERF1.[17]

[a] *Department of Cell Biology and Molecular Genetics, University of Maryland, College Park, MD 20742, USA. E-mail: carenc@umd.edu*
[b] *Biochemistry and Cellular and Molecular Biology, University of Tennessee, Knoxville, TN 37996, USA*
[c] *Animal Biosciences and Biotechnology Laboratory, USDA-ARS, Beltsville, MD 20705, USA*
[d] *Soybean Genomics and Improvement Laboratory, USDA-ARS, Beltsville, MD 20705, USA. E-mail: bret.cooper@ars.usda.gov*

† Electronic supplementary information (ESI) available: **Tables S1 and S2.** PANORAMICS[2] output of peptides and proteins. XLSX file. This includes peptide sequence matches, amino acid modifications, Mascot scores, peptide spectral counts and protein group probabilities for combined data from replicates of AIR control (S1) and ET-treated seedlings (S2). **Table S3**. Differentially accumulating proteins. XLSX file. Data include proteins with significantly different summed spectral counts, protein annotation, GOslim descriptions and presence of transmembrane domains. **Dataset S4.** Manually-annotated spectra of phosphopeptides. Zipped PDF files. See DOI: 10.1039/c1mb05159h

‡ These authors made equal contributions to this project.

Under prolonged ET treatment of several days, etiolated (dark-grown) *A. thaliana* seedlings exhibit a distinct phenotype known as the triple response, which includes hypocotyl shortening and thickening, exaggeration of the apical hook, shortening of the root and proliferation of root hairs.[18] The hypocotyls of etiolated seedlings also display ET-stimulated nutations, which are distinct oscillatory bending movements (termed "circumnutations" by Darwin).[19,20] Within the first half hour of ET treatment, etiolated seedlings exhibit a dramatic, rapid decline in growth kinetics.[21] This response appears to be independent of ET-mediated gene transcription, as it occurs even in the absence of expression of the *EIN3* and *EIL1* genes.[22] Furthermore, EIN2, EIN3 and EIL1 are subjected to proteasome-mediated degradation in the absence of ET.[17,23] However, when ET is present, these proteins are protected from degradation, accumulate and promote ET response. Likewise, but in an opposite fashion, the ETR2 ethylene receptor is degraded upon ET binding, leading to an immediate activation of signaling.[6]

These observations reveal that the ET response is regulated at a protein level in etiolated seedlings and that this proteomic regulation might precede ET-induced gene expression. Therefore, we hypothesized that ET responses may include additional levels of protein stability or degradation that may not have been previously detected by large-scale gene expression experiments or genetic screens. Given that the ET receptors and CTR1 have kinase activity, we also hypothesized that proteins involved in ET-mediated signaling pathways may be differentially phosphorylated. To test these hypotheses, we examined proteins from microsomal membrane fractions from etiolated *A. thaliana* seedlings at the onset of the triple response using Multidimensional Protein Identification Technology (MudPIT).[24] Changes in protein abundance occurred after ET treatment, and differential phosphorylation occurred in EIN2 and in other proteins with roles in ET-mediated responses.

Results and discussion

Identification of proteins by MudPIT

In 4 independent replicate experiments, *A. thaliana* wild-type seedlings were germinated in the dark for 3 days in the presence of 1-aminoethoxyvinylglycine (AVG), an ET biosynthesis inhibitor,[25] and exposed to ambient air (hereafter designated AIR) or 100 μL/L (100 ppm) ET for 3 h. In essence, AVG prevented the seedlings from responding to endogenous ET and this enabled the study of seedlings perceiving only the exogenous, external source of ET. The seedlings were quickly collected after treatment and microsomal membranes were prepared (in the presence of phosphatase and protease inhibitors). Western blotting revealed the amount of ECA1, an ER marker protein,[26] was consistent between preparations (Fig. 1). The presence of this marker also demonstrated that proteins in microsomal membranes, including ER proteins, were successfully targeted. Overall, this implied that the preparations were reasonably consistent and would be sufficient for the detection of components of ET signaling that reside in or associate with ER.

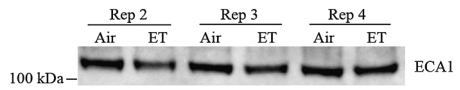

Fig. 1 Accumulation of ECA1 in microsomal membrane preparations from AIR control and ET-treated *A. thaliana* seedlings. ECA1 is a component of ER. The predicted size of unmodified ECA1 protein is 117 kDa. Replicate 1 is absent because it was used for targeted proteomics experimentation and there were insufficient amounts of it to run alongside the others when this gel was made. The blot reveals the amount of ECA1 was consistent between preparations and adds veracity to the overall consistency of the preparations.

Proteins from the microsomal membranes from each sample were digested with trypsin, and peptides were fractionated by immobilized metal affinity chromatography.[27] Fractions enriched for phosphopeptides and the remaining phosphopeptide-depleted fractions were separately analyzed on a high mass-resolution Orbitrap mass spectrometer.[28] The two sets of spectral data for each sample were pooled to make a combined spectral data set for each sample per replicate. The spectra were compared to the protein sequences deduced from the *A. thaliana* genome using Mascot,[29] and a parsimonious set of proteins at $\geq 95\%$ confidence was compiled with PANORAMICS.[30,31] Many of the same proteins were identified between replicates, but there were also some proteins not as reproducibly detected, and there were also some that were unique to a replicate (Table 1). Most likely, this variation is an effect of random sampling associated with MudPIT.[31,32] The variation between these individual *A. thaliana* samples, in terms of proteins identified and numbers of associated spectra, is generally consistent with the variation observed previously between soybean leaf replicate samples.[31]

Across all treatments and replicates, 6314 non-redundant *A. thaliana* proteins were identified overall ($\geq 95\%$ confidence, Tables S1 and S2, ESI).† Most proteins were identified with a probability greater than or equal to 0.99995 (rounded to 1 in Tables S1, S2 and S3, ESI),† and this is a direct result of Mascot search selectivity afforded by the high mass-accuracy of the Orbitrap and extensive peptide coverage for many proteins. Based on the number of proteins with probabilities in the 95–96% probability range, it was estimated that the overall protein false identification rate was less than 0.4%. Using data at The Arabidopsis Information Resource (TAIR, www.arabidopsis.org) derived from the HMMTOP membrane domain prediction program,[33] it was estimated that 21% of the proteins have transmembrane domains. This percentage is a 1.5- to 2-fold improvement over what others have reported when analyzing plant microsomal membrane preparations by MudPIT.[34,35]

EIN2, a central positive regulator of ET-signaling, was found in both AIR control and ET-treated samples (Fig. 2). No peptides were identified in the N-proximal amino acid region predicted to comprise 12 transmembrane domains; however, multiple peptides were found in the C-proximal hydrophilic region of EIN2. Other key proteins in ET signaling such as the receptors, CTR1 and TFs were not found. This suggests that these proteins were either not in the microsomal membrane preparations or were below the limits of detection. On the other hand, 2 of 3 proteins required for the final 3

Table 1 Spectra, peptides and proteins identified in four replicate experiments of ET-treated and AIR control *A. thaliana* seedlings

	AIR 1	AIR 2	AIR 3	AIR 4	ET 1	ET 2	ET 3	ET 4
Peptides $\geq$ 95%[a]	25 530	11 535	16 948	27 244	33 688	30 137	10 353	37 593
Proteins $\geq$ 95%[b]	1795	1353	1802	2860	2763	3019	1009	3775
Proteins common to 4 : 4 replicates	827	827	827	827	826	826	826	826
Proteins common to 3 : 4 replicates	1004	1004	1004	1004	908	908	908	908
Proteins unique to replicate	244	112	296	1064	382	267	59	716
Total MS2 spectra collected	379 403	228 620	276 067	367 197	327 839	304 158	271 031	379 244
Total MS3 spectra collected	372	252	363	1541	979	955	310	2030
Total summed spectral count (for $\geq$ 95% probability proteins)	35 486	14 848	21 770	37 266	43 233	37 315	14 504	47 651

[a] Mascot match probability. [b] PANORAMICS probability.

A

1 MEAEIVNVRP QLGFIQRMVP ALLPVLLVSV *GYIDPGKWVA NIEGGARFGY DLVAITLLFN*
61 *FAAILCQYVA ARISVVTGKH LAQICNEEYD KWTCMFLGIQ AEFSAILLDL TMVVGVAHAL*
121 *NLLFGVELST GVFLAAMDAF LFPVFASFLE NGMANTVSIY SAGLVLLLYV SGVLLSQSEI*
181 *PLSMNGVLTR LNGESAFALM GLLGASIVPH NFYIHSYFAG ESTSSSDVDK SSLCQDHLFA*
241 *IFGVFSGLSL VNYVLMNAAA NVFHSTGLVV LTFHDALSLM EQVFMSPLIP VVFLMLLFFS*
301 *SQITALAWAF GGEVVLHDFL KIEIPAWLHR ATIRILAVAP ALYCVWTSGA DGIYQLLIFT*
361 *QVLVAMMLPC SVIPLFRIAS SRQIMGVHKI PQVGEFLALT TFLGFLGLNV VFVVEMVFGS*
421 *SDWAGGLRWN TVMGTSIQYT TLLVSSCASL CLILWLAATP LKSASNRAEA QIWNMDAQNA*
481 *LSYPSVQEEE IER*TETRRNE DESIVRLESR **VKDQLDTTSV TSSVYDLPEN ILMTDQEIR**S
541 SPPEERELDV K**YSTSQVSSL KEDSDVK**EQS VLQSTVVNEV SDKDLIVETK MAKIEPMSPV
601 EKIVSMENNS KFIEKDVEGV SWETEEATK**A APTSNFTVGS DGPPsFRSLS GEGGSGTGSL**
661 **SR**LQGLGRAA RRHLSAILDE FWGHLYDFHG QLVAEARAK**K LDQLFGTDQK** SASSMKADSF
721 GKDISSGYCM SPTAK**GMDsQ MtssLYDsLK QQRTPGsIDS LYGLQR**GSSP SPLVNRMQML
781 GAYGNTTNNN NAYELSERRY SSLR**APSSSE GWEHQQPATV HGYQMK**SYVD NLAK**ERLEAL**
841 **QSR**GEIPTSR SMALGTLSYT QQLALALKQK SQNGLTPGPA PGFENFAGSR SISRQSERSY
901 YGVPSSGNTD TVGAAVANEK K**YSsMPDISG LSMSAR**NMHL PNNKSGYWDP SSGGGGYGAS
961 YGRLSNESSL YSNLGSRVGV PSTYDDISQS RGGYRDAYSL PQSATTGTGS LWSRQPFEQF
1021 GVAERNGAVG EELRNRSNPI NIDNNASSNV DAEAKLLQSF RHCILKLIKL EGSEWLFGQS
1081 DGVDEELIDR VAAREKFIYE AEAREINQVG HMGEPLISSV PNCGDGCVWR ADLIVSFGVW
1141 CIHRVLDLSL MESRPELWGK YTYVLNRLQG VIDPAFSKLR TPMTPCFCLQ IPASHQRASP
1201 TSANGMLPPA AKPAKGKCTT AVTLLDLIK**D VEMAISCRK**G RTGTAAGDVA FPKGKENLAS
1261 VLKRYKRR**LS NKPVGMNQDG PGsR**KNVTAY GSLG

B

AIR # reps observed (4 max.)	AIR spectral counts	EIN2 peptide sequences found by MS2	ET spectral counts	ET # reps observed (4 max.)
1	2	ERLEALQSR	1	1
1	6	DVEMAISCRK	10	2
1	2	KLDQLFGTDQK	6	3
2	5	TPGSIDSLYGLQR	nf	0
1	3	TPG*SIDSLYGLQR	nf	0
1	3	Y†S*SMPDISGLSMSAR	nf	0
0	nf	SLSGEGGSGTGSLSR	1	1
0	nf	LSNKPVGMNQDGPGSR	5	2
1	2	LSNKPVGMNQDGPG*SR	nf	0
1	1	GMD*SQM*T*S*SLYD*SLK	nf	0
0	nf	GMD*SQM*TS*SLYD*SLKQQR	1	1
1	6	YSTSQVSSLKEDSDVK	1	1
0	nf	AAPTSNFTVGSDGPPSFR	1	1
3	7	AAPTSNFTVGSDGPP*SFR	nf	0
0	nf	APSSSEGWEHQQPATVHGYQMK	3	1
1	6	VKDQLDTTSVTSSVYDLPENILMTDQEIR	6	2

na, not applicable; nf, not found; *, phosphorylation found on the following amino acid; †, alternative site of phosphorylation on the following amino acid

Fig. 2 EIN2 peptides identified by MudPIT. (A) Protein sequence of EIN2. Sequences identified by MudPIT are in bold, phosphorylated amino acids in lower-case underlined bold, and the predicted transmembrane region italicized. (B) EIN2 peptides found between AIR control and ET treated samples.

enzymatic steps of ET biosynthesis were found; nine isoforms of S-adenosyl methionine transferase (SAM synthetase) and five 1-aminocyclopropane-1-carboxylic acid (ACC) oxidases were observed. These findings suggested that some proteins involved in ET signaling were successfully isolated.

Protein accumulation changes that correlate with ET treatment

Relative amounts of proteins identified by MudPIT can be estimated using the summed spectral counting method, and summed spectral count differences between samples can be distinguished statistically.[31,36–38] Spectral data sets from the 4 replicate experiments for each treatment were pooled because we and others have demonstrated that this reduces random sampling effects associated with MudPIT and increases the statistical confidence associated with reproducible detection of proteins.[31,36] We examined the summed spectral counts of 3814 proteins found in both ET-treated and AIR control seedlings and statistically distinguished 304 that were different [1.0% false discovery rate (FDR); Fig. 3; Table S3, ESI].† Nearly two-thirds of the proteins exhibited changes greater than 2-fold (fold-change values are Log base 2 in Table S3, ESI).† This suggests that many changes were robust. Fifty-six percent of the proteins were observed in at least 6 of the 8 total AIR and ET samples (Table S3, ESI).† This reveals that most of the differentially accumulating proteins were reproducibly detectable. These differentially accumulating proteins will be described in the following paragraphs. As for the proteins without significantly different spectral counts, either they had similar abundances or more data is needed to determine if statistical differences exist. Some interesting information can still be taken from the set of proteins without significantly different spectral counts. For example, ECA1, the ER marker protein that appeared in Fig. 1 to be at equivalent amounts in the microsomal preparations from the AIR control and ET-treated seedlings, did not have statistically different spectral counts. Thus, the spectral count data can be construed to be consistent with the Western blot data in this case. EIN2, a central regulator of ET signaling that was found in both ET-treated and AIR control seedlings, also did not have statistically different spectral counts. These results are different from those in a previous report that showed by Western blot a small increase in EIN2 protein level in 3-day-old *A. thaliana* WT seedlings after 4 h of 10 ppm ET exposure, but not after 1 h.[23] It is possible that the amount of EIN2 increases between 3–4 h after exposure to ET or that changes in EIN2 abundance are different under 10 ppm ET exposure compared to 100 ppm ET exposure.

Among the 304 proteins with significantly different spectral counts, there were 189 proteins with increased counts and 115 with decreased counts (Table S3, ESI).† Assignment to Gene Ontology (GO) molecular-function GOslim terms[39] revealed generalized differences between the two sets (Fig. 4). There were more proteins with increased counts upon ET-treatment that were classified as "nucleotide binding," "transferase activity" and "other enzyme activity" compared to proteins with decreased summed counts, and fewer proteins classified as "structural molecule activity" and "transporter activity." Except for ribosomal proteins classified as "structural molecule activity" (which will be discussed later), this gross classification of molecular function provided little insight about the proteomic effects associated with ET response, so a comprehensive investigation of the proteins discovered was performed to reveal germane insight to their specific, potential roles in ET biology.

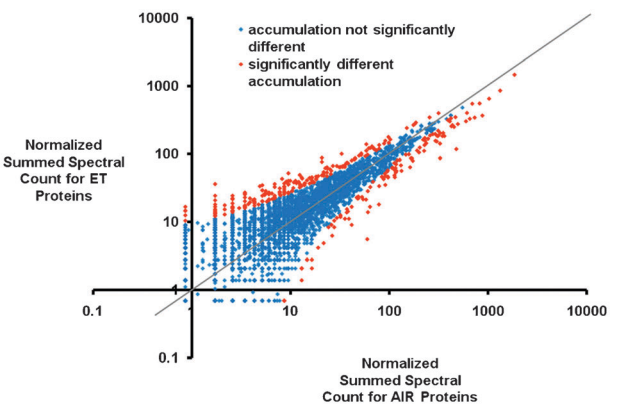

Fig. 3 Summed spectral counts of proteins in AIR control and ET-treated *A. thaliana* seedlings. Normalized values for summed spectral counts are plotted on Log_{10} axes. A G-test was used to determine if summed spectral counts for each protein differed between treatments and the FDR was estimated to be 1.0%. 304 proteins with significantly different accumulation after ET treatment are in red and 3510 proteins without significantly different accumulation are in blue.

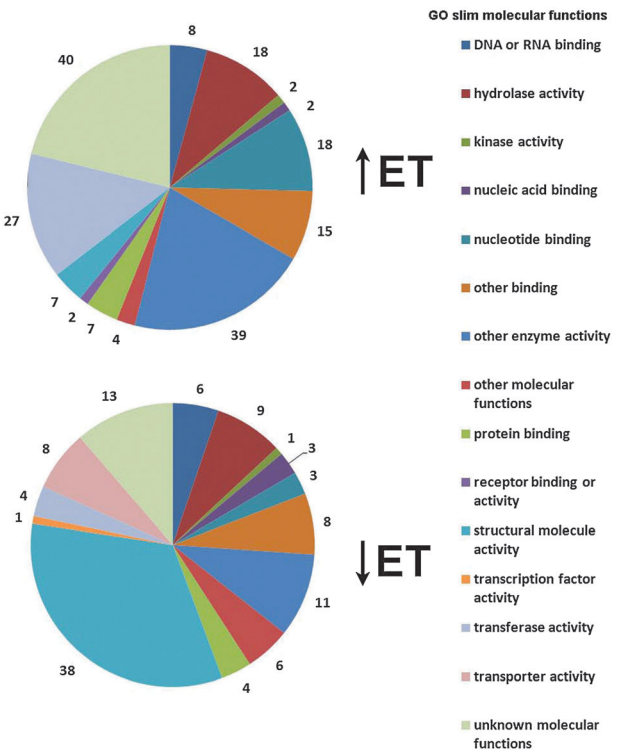

Fig. 4 Classification of proteins exhibiting differential summed spectral counts after ET-treatment. The charts show GOslim molecular function categorizations for 189 proteins with significantly increased counts upon ET treatment (↑ET) and 115 proteins with significantly decreased summed spectral counts upon ET treatment (↓ET).

For example, by evaluating the enzymes specifically involved in ET biosynthesis, we could determine the effect of exogenous ET application on this pathway. There were seven SAM synthetases found in both AIR control and ET-treated seedlings, but there were no significant differences in their summed spectral counts. These findings are consistent with the fact that SAM synthetase, while required for ET biosynthesis, is not a key regulated component. Rather, under stress conditions and in response to ET, ACC oxidase transcriptional rates and enzymatic activity increase, which are indicative of a positive feedback loop for ET biosynthesis during seedling germination.[40–44] In our experiment, 2 ACC oxidase isoforms had greater summed spectral counts upon ET-treatment, consistent with positive-feedback. The data is not consistent, however, with negative-feedback regulation of ET (autoinhibition) observed in other circumstances.[18]

Other potential effects on seedling biology could also be deduced by the protein accumulation changes. The summed spectral counts for α-tubulin proteins TUA1, TUA6 and TUA2/TUA4 and TUA3/TUA5 (the slash denotes identical proteins encoded by different genes[45]) were significantly increased after ET treatment. The α-tubulins and β-tubulins make up microtubules that are critical for plant cell morphogenesis and nuclear reorganization.[45] Other proteins like RANGAP1 and TON1b that associate with microtubules during interphase and preprophase[46,47] also had increased spectral counts after ET treatment. These data suggest that ET treatment leads to microtubule metabolic changes that affect cellular morphology or nuclear division, or both. Supporting the former is the concomitant increase in 18 enzymes involved in polyhexose synthesis. One of these was CESA6, a cellulose synthase involved in microtubule orientation.[48] Hence, ET appears to affect proteins coordinating cell morphological change.

PAD2, a protein important for pathogen defense and for moderating oxidative stress by catalyzing the rate limiting step of glutathione (GSH) production,[49] also had increased counts as a result of ET treatment. ET perception has been linked to increased PAD2 (GSH1) enzyme activity and GSH levels.[50,51] Thus, the increase in PAD2 suggests a proteomic shift favoring an increased response to a real or perceived potential for oxidative stress. Supporting that notion are the observations that VTE1, a key enzyme in the production of the antioxidant tocopherol,[52] and 6 other proteins facilitating the oxidative stress-response such as glutathione S-transferase (GST6) all had significantly increased spectral counts upon ET treatment. Proteins involved in other stress responses also appeared to have increased spectral counts, namely 9 proteins annotated as "dehydration-responsive." TAIR annotation suggests that these 9 proteins may be localized to the Golgi bodies, suggesting an influence of ET upon this organelle. All together, it appears that ET perception leads to oxidative stress response at a proteomic level.

The influence of ET on a number of additional Golgi body proteins suggests an overall effect of proteins involved in vesicle secretion. Twelve proteins involved in vesicle secretion including clathrin, SEC24A, a coat protomer complex II (COPII) protein,[53] VPS45 and similar proteins controlling vesicle trafficking,[54] and vesicle tethering/receptor proteins such as N-ETHYLMALEIMIDE SENSITIVE FACTOR[55] had increased counts. Biological processes that are linked to vesicle secretion include fatty acid/lipid production and fatty acid oxidation in the peroxisome. There were 10 proteins such as lipoxygenases and lipid acyl hydrolases, with increased counts. One acyl-CoA synthase with increased counts, AT5G27600, interacts with peroxisomal receptor PEX5,[56] which also had increased abundance. PEX11D, PEX11E and BIGYIN, which control peroxisome proliferation and fission,[57,58] all had increased counts as well. Few proteins involved in the aforementioned processes had decreased summed spectral counts after ET treatment. Hence, it appears that increases in accumulation of proteins with roles in vesicle formation, cargo, recognition, interaction with peroxisomes and fatty acid metabolism are part of the ET response in seedlings.

ET and brassinosteroid (BR)-mediated hormonal processes are for the most part transcriptionally distinct,[59] but there is evidence of cross-talk between these processes, *e.g.* they both are involved in apical hook formation in growing seedlings.[60] Thus, it could be presumed that there may be some proteomic overlap between ET and BR-mediated responses. Exogenous application of a BR-analog to BR-deficient *det2 A. thaliana* seedlings caused increased accumulation of TUA3, TUA4, TUA6 and UDP-xylose synthase between 2 and 6 h after treatment.[61,62] In our studies, there were similar increases in these proteins in ET-treated seedlings. This evidence supports proteomic crossover in ET- and BR-mediated cellular morphogenesis. However, other evidence supports an antagonistic relationship. Our experiments showed an increase in the ET-forming ACC oxidase after ET treatment, but the same protein had decreased accumulation after BR-analog treatment in *det2* seedlings.[61] This opposite response suggests that BR signaling represses ET response. In fact, increases of patellins, jacalin, BiP2, a myrosinase-associated protein, and *det2*-suppressing DREPP, along with decreases of phosphoenolpyruvate carboxykinase and GST6 that were particular to BR-analog treated *det2* mutants were completely opposite in ET-treated seedlings. Other related proteins like ER-associated BiP1, another jacalin and other myrosinase-associated proteins also had decreased accumulation in ET-treated seedlings. A beta-glucosidase (AT1G66270) that associates with ER and other jacalins[63] had decreased accumulation in ET-treated seedlings as well. Thus, it appears that some proteomic responses governed by ET and BR responses overlap while others may be antagonistic. It is possible that the antagonism is controlled by various checkpoints that have not been completely elucidated. For example, DWF1, an enzyme involved in an early step of BR biosynthesis,[64] had increased spectral counts in ET-treated seedlings. Curiously, overexpression of DWF1 by itself does not provide a hyper-morphic BR phenotype.[64] Instead DWF1 regulatory activity on BR biosynthesis is likely controlled by available calmodulin.[64] Interestingly, in ET-treated seedlings there was a decrease in calmodulin and the calcium-binding DREPP protein.[65] Thus, calmodulin could be a checkpoint that separates some ET- and BR-mediated proteomic responses.

Several other proteins had decreased spectral counts upon ET-treatment. The *A. thaliana* protein RHD1, a UDP-glucose 4-epimerase whose transcript was previously shown to decrease

in roots treated with ET,[66] had decreased spectral counts in ET-treated seedlings. Another protein that had lower summed spectral counts in ET-treated seedlings was plasma membrane-associated, cold temperature-induced lipocalin (AtTIL1), a protein that also protects against oxidative stress.[67] Over-expression of the AtTIL1 gene in transgenic plants caused delayed flowering and delayed senescence,[67] a phenotype similar to that observed for ET-insensitive mutants such as *etr1* and *ein2*.[68] Thus, ET may decrease AtTIL1 to promote the ET response. Finally, 35% of the proteins with decreased summed spectral counts were ribosomal proteins (GO: structural molecule activity; Fig. 4). There were only 4 ribosomal proteins among those with increased spectral counts. This suggests that ET-treatment affected the abundance of these ribosomal proteins.

Spectral counting of targeted proteins

The masses for peptides of three proteins were specifically targeted in MudPIT and dynamic exclusion was turned off to see if the targeted counts in individual replicate experiments were consistent with the summed spectral counts for the respective proteins in the cumulative data from all 4 experiments. The peptide WYEIASFPSR for AtTIL1 was associated with 19 876 spectral counts in a sample from AIR control seedlings and 10 061 spectral counts in the analogous sample from ET-treated seedlings. This near 2 : 1 ratio is consistent with the significantly different summed spectral count ratio for all 4 MudPIT experiments (187 AIR/92 ET). The peptide KIVCDPSYLPNK of ATGDI2 (a RAB GDP dissociation inhibitor) had counts of 30/60 and 70/110 in targeted experiments of 2 of the replicate samples from AIR control/ET-treated seedlings. The targeted peptide count ratios of 1 : 2 and 1 : 1.6 were consistent with the summed spectral counts from all 4 MudPIT experiments (35 AIR/63 ET summed counts or 1 : 1.8). Finally, the peptide HIANLAGNPK from LOS2 had 220/299 and 268/309 counts in targeted experiments of 2 of the replicate samples from AIR control/ET-treated seedlings. Once again, the targeted count relationships were similar to the summed spectral count relationships for all 4 MudPIT experiments (152 AIR/178 ET). Hence, it appears that the targeted peptide spectral counts from individual replicate experiments mirrored the summed spectral count data from 4 replicates for the respective peptides/proteins.

Phosphorylation upon ET treatment

Several steps were taken to specifically identify phosphorylated peptides in these MudPIT experiments. First, samples were enriched for phosphopeptides by exploiting the affinity properties of gallium.[27] Next, the mass spectrometer was configured to perform MS^3 on MS^2 ions exhibiting neutral loss of phosphoric acid.[69] Finally, Mascot was configured to consider phosphorylation as a variable mass modification of S and T, and PANORAMICS[2] was used to analyze Mascot data and make use of corroborating MS^3 spectra to find sites of dehydration associated with phosphoric acid neutral loss.[30] To generally demonstrate these measures were effective, an Ions score cut-off of 30 was arbitrarily chosen to assess the distribution of phosphopeptides found between the two data sets. There were 237 unique phosphopeptides distributed among 220 non-redundant proteins in AIR data sets, and there were 307 unique phosphopeptides distributed among 294 proteins in ET data sets (Table S1 and S2, ESI).† Thus, similar numbers of phosphopeptides were found between the two data sets.

The amino acid positioning for phosphate moieties was clearly ascertainable from the MS^2 fragmentation information only when there was an equal number of potential sites for moieties detected, if no neutral loss of phosphoric acid occurred in that position resulting in a mass shift of +80 Da for the respective fragment ion in the peptide spectrum, or if the phosphopeptide ion was +3 charged.[70,71] However, in some cases, Mascot matched a phosphorylated peptide to a MS^2 spectrum of a +2 charged ion and assigned phosphate moieties to multiple positions in the peptide. Thus, it was sometimes difficult to determine the exact position of phosphorylation based on a single spectrum, especially since it was possible that gas-phase rearrangements for phosphate moieties on peptides with multiple possible positions led to a convoluted spectrum representing a mixture of these molecular rearrangements.[71] A recent report that investigated the rates of gas-phase rearrangements of model +2 charged phosphopeptides suggested that the phosphorylation position attributed to the highest scoring peptide is most likely to be correct.[70] So, we designed a decision tree for confidently identifying sites of phosphorylation (Fig. 5). To evaluate site positioning for phosphopeptide sequence-spectrum matches, we considered the number of moieties and the number of potential sites for phosphorylation, the Mascot Ions score magnitude and the probability of the sequence-spectrum match (the Mascot probability is the relationship between the Ions and the Identity score[72]), the peptide charge state, +80 Da mass shifts (meaning no neutral loss but phosphorylation mass gain at an amino acid position), phosphoric acid neutral losses (leading to −18 Da mass loss at S/T^{30}) and corroborating neutral loss-generated MS^3 spectra. This information was used to assign high, moderate or low confidence for phosphorylation positioning to the specific peptides listed in Table 2. Manual annotations for these spectra are provided as proof of phosphorylation and site positioning (Dataset S4, ESI).†

EIN2, a central positive regulator of ET signaling, was found to be phosphorylated. Phosphorylation was observed at S positions 645, 739, 743, 744, 748, 757 and 1283, and either 923 or 924 and at T 742 (Fig. 2, Table 2, Dataset S4, ESI).† Phosphorylation at position S 645 was identified with a high degree of confidence (Fig. 2 and Table 2). This residue is conserved in EIN2 homologues from castor bean, poplar, grape, peach, barrel medic, petunia, tomato, rice, sorghum and maize, which implies the site is significant. It was difficult to distinguish between phosphorylation at position S 923 and S 924 (Fig. 2 and Table 2), however residue S 924 exhibited the most conservation in EIN2 homologs from castor bean, poplar, grape, peach, barrel medic, petunia, tomato, rice, sorghum and maize. The other sites of phosphorylation were identified with varying degrees of confidence and also exhibited varied degrees of conservation in EIN2 homologues with the least amount of conservation observed at residue S 1283.

Because we evaluated sample fractions enriched for phosphopeptides and also the remaining depleted fractions from

High confidence

Equal # sites for equal # phosphorylation modifications (Mascot match probability ≥ 95%).

If not equal:

+2 or +3 charged parent ion,
MS²: if no neutral loss of -98 Da, site determining ions for S/T +80 Da (Mascot match probability ≥ 95%);
+3 charged parent ion,
MS²: if neutral loss of -98 Da, site determining ions for S/T -18 Da (Mascot match probability ≥ 95%) or no site determining ions (positions are deduced) plus a -98 Da triggered MS³ spectrum with corresponding ions;
+2 charged parent ion,
MS²: if neutral loss -98 Da, site determining ions for S/T -18 Da (Mascot match probability ≥ 95%) plus a -98 Da triggered MS³ spectrum with corresponding site determining ions.

Moderate confidence

If not equal:

Peptides meeting high confidence criteria but Mascot match probability ≥ 90%

or

+2 or +3 charged parent ion,
MS²: if no neutral loss of -98 Da, no site determining ions (positions are deduced) for S/T +80 Da (Mascot match probability ≥ 95%);
+3 charged parent ion,
MS²: if neutral loss -98 Da, no site determining ions (positions are deduced) for S/T -18 Da (Mascot match probability ≥ 95%);
+2 charged parent ion,
MS²: if neutral loss -98 Da, site determining ions for S/T -18 Da (Mascot match probability ≥ 95%).

Low confidence

If not equal:

Peptides meeting moderate confidence criteria but Mascot match probability ≥ 85%

or

+2 charged parent ion,
MS²: if neutral loss -98 Da, no site determining ions (positions are deduced) for S/T -18 Da (Mascot match probability ≥ 95%).

Fig. 5 Confidence indicators for amino acid positioning of phosphorylation.

both ET-treated and control seedlings, we were able to examine whether differential phosphorylation occurred after ET treatment. EIN2 appeared to be differentially phosphorylated, even though the whole protein did not exhibit differential accumulation after ET treatment (Table 3, Fig. 2). For example, the EIN2 phosphopeptide AAPTSNFTVGSDGPP*SFR (* indicates phosphorylation of the following amino acid), a peptide with the most conserved phosphorylated S site, was found in 3 out of 4 biological replicates for AIR control seedlings (Table 3, Fig. 2). The non-phosphorylated analog was not found in AIR control seedlings; however, in ET treated seedlings, only the non-phosphorylated analog was found. Similarly, the phosphopeptide LSNKPVGMNQDPG*SR was found in AIR data sets while the non-phosphorylated version was not; only the non-phosphorylated version was present in ET data sets. Finally, two other phosphopeptides were in AIR data sets but not in ET data sets in any form. Together, these data suggest that EIN2 phosphopeptides were more readily detected in AIR control seedlings compared to ET-treated seedlings. In other words, the data suggest that EIN2 exists in

Table 2 Evidence for amino acid positioning of phosphorylation on *A. thaliana* peptides

Protein	Description	Phosphopeptide sequence matched	Mascot ions score	Mascot match probability	Evidence for position determination‡,Π	Confidence in position assignment‡
AT5G03280	EIN2	AAPTSNFTVGSDGPP*SFR	73.0	>99%	MS2: +2 charge; y ion found for S16 [+80]; MS3: S16 [−18]	High
AT5G03280	EIN2	LSNKPVGMNQDGPG*SR	26.7	93%	MS2: + 2 charge; deduced S15 [+80]	Low
AT5G03280	EIN2	TPG*SIDSLYGLQR	35.6	>99%	MS2: +2 charge; b–y ions found for S4 [−18]; MS3: y ion found for S4 [−18]	High
AT5G03280	EIN2	Y†S*SMPDISGLSMSAR	29.9	97%	MS2: +2 charge; b ion found for S3 [−18] but 2nd ranked match of deduced S2 [−18] had Ions score of 29.7	Moderate/ ambiguous
AT5G03280	EIN2	GMD*SQM*TS*SLYD*SLKQQR	17.3	87%	MS2: +3 charge; deduced S4, T7, S9, S13 [+80]; multiply-phosphorylated peptides ionize poorly	Low
AT5G03280	EIN2	GMD*SQM*T*S*SLYDSLK	14.2	95%	MS2: +3 charge; b ion found for S4 [−18]; deduced T7, S8, S9 [−18]; multiply-phosphorylated peptides ionize poorly	Moderate
AT5G19770/ AT5G19780	Alpha-tubulin	IHFMLSSYAPVI*SAAK	42.8	>99%	MS2: +2 charge; y ion found for S13 [+80]	High
AT2G39130	Amino acid transporter	FGSSFL*SSGLIR	50.9	>99%	MS2: +2 charge; y ion found for S7 [+80]	High
AT2G39130	Amino acid transporter	LSSQGLL*SPIPSR	51.1	>99%	MS2: +2 charge; b and y ions found for S8 [+80]	High
AT2G39130	Amino acid transporter	L*SSQGLL*SPIPSR	31.7	97%	MS2: +2 charge; b and y ions found for S8 [−18]; deduced S2 [−18]; MS3: b and y ions found for S8 [−18]; y ion found for S3, so S2 [−18]	High
AT5G64330	NPH3	MSGQESHDI*S*SGGEQAGVDHPPPR	26.7	95%	MS2: +3 charge; deduced S10, S11 [+80]; MS3: b ion found for S10 [−18]; deduced S11 [+80]	High
AT5G64330	NPH3	MSGQESHDIS*SGGEQAGVDHPPPR	36.3	>99%	MS2: +3 charge; b and y ions found for S11 [−18]; MS3: y ion found for S11 [−18]	High
AT5G64330	NPH3	LLEHFLVQEQTEGS*SPSR	36.1	>99%	MS2: +3 charge; y ion found for S15 [+80]	High
AT5G64330	NPH3	LLEHFLVQEQTEG*SSPSR	37.8	>99%	MS2: +2 charge; deduced S14 [+80]	Moderate
AT4G12770	Heat shock protein binding	GGSFE*S*SRP*S*SR	12.4	85%	MS2: +3 charge; deduced S6, S7, S10, S11 [−18]; multiple-phosphorylated peptides ionize poorly	Low
AT5G49890	Anion channel	KI*SGILDDGSVGFR	89.5	>99%	MS2: +2 charge; b and y ions found for S3 [−18]; MS3: y ion found for S3 [−18]	High
AT1G45688	Unknown	RPVYYVQ*SPSR	24.5	90%	MS2: +2 charge; b ion found for S8 [−18]; MS3: b ion found for S8 [−18]	Moderate

*, the following amino acid is phosphorylated; †, alternative site of phosphorylation on following amino acid; ‡, see Fig. 5 for confidence indicators; Π, for MS2 spectra, if there is no neutral loss of phosphoric acid, then site specific ions for S/T consider phosphorylation [+80], but if there is neutral loss of phosphoric acid, then site specific ions for S/T consider the loss of water [+80−98 = −18]).[30] For MS3, dehydrated S/T is the likely result of neutral loss of phosphoric acid in the prior MS2 event.[30]

a phosphorylated state in the absence of ET signaling and that ET treatment leads to analogous non-phosphorylated EIN2 peptides. The lack of detection of some EIN2 phosphopeptides in ET-treated seedlings is unlikely to be a product of under-sampling because 7 out of 10 EIN2 peptides identified in AIR control seedlings were also found in ET-treated seedlings, and the largest non-phosphorylated peptide was observed an equal number of times across the treatments (Fig. 2B).

Other peptides from other proteins also exhibited differential phosphorylation as a result of ET treatment (Tables 2 and 3). IHFMLSSYAPVISAAK of TUA3/TUA5 was found only in the non-phosphorylated form across all 4 AIR replicate data sets, but both non-phosphorylated and phosphorylated forms were in the ET data sets. The phosphorylated FGSSFLSSGLIR peptide from protein AT2G39130 was found more often in the ET data sets. For another peptide in AT2G39130, the singly-phosphorylated and non-phosphorylated forms were found in AIR. However, in ET-treated seedlings MS^3 confirmed that the peptide was phosphorylated twice. Double phosphorylation and MS^3 were not observed in AIR seedlings. The additional site of phosphorylation in AT2G39130 that was observed under ET-treatment is conserved in homologues in grape, poplar, castor bean, rice, sorghum and maize, but the former site was not conserved, which suggests that the additional site of phosphorylation is significant. NON-PHOTOTROPIC HYPOCOTYL 3 (NPH3),

Table 3 *A. thaliana* peptides showing differential phosphorylation after ET treatment

Protein	Description	Peptide	Spectral count non-phos/phos AIR	Spectral count non-phos/phos ET	Replicates observed (4 max.) AIR	Replicates observed (4 max.) ET
AT5G03280	EIN2	AAPTSNFTVGSDGPP*SFR	0/7	1/0	3	1
		LSNKPVGMNQDGPG*SR	0/2	5/0	1	2
		TPG*SIDSLYGLQR	5/3	0/0	1	0
		Y†S*SMPDISGLSMSAR	0/3	0/0	1	0
AT5G19770/ AT5G19780	Alpha-tubulin	IHFMLSSYAPVI*SAAK	10/0	34/6	4	4
AT2G39130	Amino acid transporter	FGSSFL*SSGLIR	3/1	2/5	2	4
		LSSQGLL*SPIPSR	3/2	2/0	1	3
		L*SSQGLL*SPIPSR	-/0	-/2	—	—
AT5G64330	NPH3	MSGQESHDI*S*SGGEQAGVDHPPPR	1/0	2/2	1	1
		MSGQESHDIS*SGGEQAGVDHPPPR	-/0	-/4	—	—
		LLEHFLVQEQTEGS*SPSR	0/0	1/6	0	1
		LLEHFLVQEQTEG*SSPSR	0/0	0/1	0	—
AT4G12770	Heat shock protein binding	GGSFE*S*SRP*S*SR	4/0	4/4	1	1
AT5G49890	Anion channel	KI*SGILDDGSVGFR	2/5	1/9	2	2
AT1G45688	Unknown	RPVYYVQ*SPSR	6/0	8/5	1	3

*, the following amino acid is phosphorylated; †, alternative site of phosphorylation on following amino acid; -, data for this peptide form is redundant and is subsumed by the data for the related peptide form listed above it (*e.g.* the counts for non-phosphorylated MSGQESHDISSGGEQAGVDHPPPR are only listed once while there are different counts for the phosphorylated forms).

a plasma membrane-bound signal transducer involved in seedling phototropic response to blue light,[73] also exhibited differential phosphorylation. One phosphopeptide, LLEHFLVQEQTEGS*SPSR, was only observed in ET-treated seedlings, and the site of phosphorylation was conserved in homologues in grape, poplar, castor bean, maize and rice. Three other proteins also had peptides that exhibited differential phosphorylation. These proteins include a membrane anion channel protein that contributes to nitrate and chloride homeostasis,[74] a predicted heat shock binding protein, and a protein of unknown function. These proteins did not have differential summed spectral counts at the protein level despite showing differential phosphorylation at the peptide level.

It bears noting that while EIN2 appeared to be phosphorylated prior to ET treatment, these other proteins appeared to be phosphorylated after ET treatment (Table 3). Thus, these proteins may be regulated through a different ET-mediated process, possibly by other kinases regulated by ET perception. Our data included 4 kinases (AT5G49760, AT5G10020, AT2G26730, AT3G17840) with leucine-rich repeat, receptor and transmembrane domains, and these proteins exhibited increased accumulation upon ET treatment (Table S3, ESI).† Thus, it may be possible that increasing amounts of these kinases help drive phosphorylation events after ET-treatment.

Evaluation of plant phenotypes with mutant genes

Based on protein accumulation shifts and peptide phosphorylation state changes for TUA3/5 after ET treatment, we hypothesized that *tua3/5* mutants might display altered ET-response phenotypes related to cellular morphological change. TUA3 and TUA5 proteins have the same primary amino acid sequence, but their cognate genes have tissue-specific transcriptional activities.[45] Therefore, we examined plants with separate mutations in homozygous recessive $tua3^{D205N}$ and $tua5^{D251N}$ lines.[75] ET-treated *tua3* mutants had growth response kinetics indistinguishable from ET-treated wild-type seedlings (Fig. 6A). However, *tua3* mutants had altered nutations (Fig. 6B). ET-treated wild-type seedlings nutated with an average peak amplitude of approximately 18° while ET-treated *tua3* mutants nutated with an amplitude of approximately 7°. Examination of the ET-treated *tua5* mutant revealed no changes in either growth response kinetics (data not shown) or nutational amplitude (Fig. 6B). Therefore, TUA3 is involved in ET-mediated nutation, but not growth inhibition upon application of ET and not growth recovery when ET is removed.

Conclusion

Our data revealed for the first time that EIN2, a major regulator of ET-mediated response, is phosphorylated. In fact, our data suggest that EIN2 is phosphorylated when ET is absent but is less phosphorylated in the presence of ET. Thus, it is possible that the activity of EIN2 could be regulated by differential phosphorylation. Qiao *et al.* reported that EIN2 is synthesized but targeted for degradation in the absence of ET, thus preventing an ET response.[23] Furthermore, the ET response is repressed by CTR1 kinase activity, but activated when CTR1 kinase activity is turned off.[10] Thus, in the absence of ET and in the presence of active kinases, phosphorylation of EIN2 may serve as a regulatory mechanism that targets EIN2 for degradation to prevent the ET-response, whereas in the presence of ET and absence of active kinase, EIN2 is specifically dephosphorylated and/or newly synthesized EIN2 is no longer specifically phosphorylated resulting in the activation of ET response. The exact regulatory effects of phosphorylation upon EIN2 and the identities of the upstream kinases will now need to be determined.

Our data also revealed for the first time that there are significant shifts in the abundance of many proteins upon

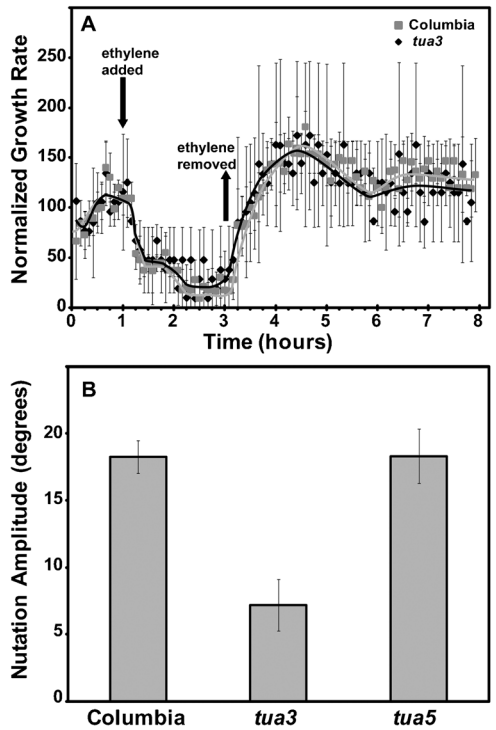

Fig. 6 Growth responses in *A. thaliana* Columbia (wild-type), and *tua3* and *tua5* mutants. (A) Growth inhibition and recovery kinetics. Seedlings were allowed to grow in ET-free air for 1 h prior to the introduction of ET. ET was removed 2 h later. (B) The amplitude of nutational bending was measured in the hypocotyls of seedlings treated with ET for 24 h.

ET treatment. Proteins with increased accumulation included those involved in ET biosynthesis as part of a positive feedback loop, and proteins involved in cell morphogenesis, oxidative stress and vesicle secretion. Some of these processes have been implicated in ET responses by alternative means of biological study but the underlying proteins had not been discovered.[42,51,76,77]

There were also proteins that exhibited decreased accumulation upon ET-treatment, including those inversely regulated by BR and ribosomal proteins. The reduction of ribosomal proteins suggests that ET treatment causes a profound shift in cellular metabolism such that the cell promptly shunts to the proteasome pre-ET-treatment ribosomal proteins, mRNA and nascent polypeptides no longer needed for the post ET-treatment cellular environment. It is already known that ETR2 and EBF1/2 are subject to degradation upon ET perception,[6,17] genes involved in protein degradation exhibit ET-induced expression,[78] and proteasome-mediated degradation responses occur during other hormonal responses.[79–81] Thus, the post-ET seedling may undergo rapid proteomic turnover and this may explain a drop in growth rate kinetics in ET-treated seedlings.[21] At the same time, not all proteins are rapidly degraded as it is known that ET-treatment increases the protein stability of EIN2, EIN3 and EIL1.[17,23,82] Thus, increased protein accumulation that we observe might not necessarily be due to novel synthesis in all cases but rather to increased protein stability or increased migration to membranes of specific ET-regulated proteins.

Most of the proteins identified have never before been firmly linked to ET-mediated responses. We have sought to confirm the data set by comparing it to other systems biology data sets. However, our proteomic data exhibited very little overlap with ET-mediated gene expression changes[40,59]—the only notable similarity being that both ACC oxidase gene expression and protein accumulation increase during ET-mediated response. Different experimental conditions could explain the incongruence. However, evidence already shows that early ET-induced growth changes are independent of gene transcription.[22] So, there is little expectation for great overlap between gene expression and proteomic changes at the time point we examined. Thus, to begin to validate proteins in our dataset, we have used reverse-genetics to study the phenotypes associated with mutant alleles. Our confirmation of a diminished ET-mediated nutation phenotype in *tua3* seedlings reveals that α-tubulin plays a role in morphological dynamics induced by ET.

On a historical note, Charles Darwin was always perplexed in the apparent rapid diversification of flowering plants according to the fossil records during his time, which challenged his theory of gradual evolution.[83] Perhaps looking for adaptations that would support his notion, he described in detail in one of his last publications before his death many aspects of nutation in numerous plant species.[19] He hypothesized about nutation: "through its modification that many highly beneficial or necessary movements have been acquired."[19] Based on our proteomics research, we now know that TUA3 is one genetic determinant of nutation and that mutation of TUA3 leads to a variation of form and movement, as Darwin predicted.

Experimental

Plant material

Arabidopsis thaliana wild-type Columbia (Col-0) seeds were from Lehle Seeds (Round Rock TX, USA), and $tua3^{D205N}$ and $tua5^{D251N}$ seeds[75] were provided by Dr Takashi Hashimoto (Nara Institute of Science and Technology, Nara, Japan).

ET treatment

For each treatment, approximately 270 mg Col-0 seeds (~4800 ct.) were sown on 3 plates with 0.8% (w/v) agar, 1× Murashige and Skoog medium and 5 μM AVG (Sigma-Aldrich, St. Louis, MO). Sown plates were placed in two identical airtight, light-tight, black acrylic chambers (3 plates each) (PlasLabs, Lansing, MI). The chambers were incubated for 3 days at 4 °C to cold-stratify the seeds. The sown plates were removed from the acrylic chambers and incubated in a plant growth chamber at 20 °C where they were exposed to 6 h visible light to facilitate germination. The sown plates were placed back into the acrylic chambers in complete darkness at 20 °C for 66 h by which point germination occurred. Continuing in complete darkness, one acrylic chamber was subsequently injected to reach a final concentration of 100 μL/L (100 ppm) ET gas (Specialty Gases of America, Toledo, OH). The other acrylic chamber was not injected with ET, and these seedlings are considered "non-treated" controls (AIR). After 3 h of treatment, the

seedlings were harvested by gently scraping the surface of each plate with blunt forceps, were flash frozen in liquid nitrogen and stored at −80 °C. Harvesting took less than 1 min for each plate and was carried out under green light conditions for visibility. The procedure was performed 4 separate times.

Protein preparation

To enrich for microsomal membranes, approximately 3 g frozen, treated seedlings were ground into a powder in liquid nitrogen and homogenized in extraction buffer [50 mM Tris-HCl, pH 7.5, 330 mM sucrose, 5 mM EDTA, 5 mM DTT, 1 mM PMSF, 1% proteinase inhibitor (P9599, Sigma-Aldrich), and 1% phosphatase inhibitors (P2850 and P5726, Sigma-Aldrich)] with a ground-glass homogenizer. The homogenate was filtered through two layers of Miracloth (Merck, Darmstadt, Germany) and centrifuged at 10 000 × *g* for 10 min. The supernatant was centrifuged at 60 000 × *g* for 45 min. The pellet was dissolved in 500 μL buffer [8 M urea/100 mM Tris-HCl, pH 8.0, and 2% dodecyl-β-maltoside (Sigma-Aldrich)]. Proteins were precipitated in 25% trichloroacetic acid, washed in acetone, and resolubilized in 8 M urea/100 mM Tris-HCl, pH 8.0. Protein concentrations were estimated by bicinchoninic assay (Pierce, Rockford, IL, USA). About 600 μg protein from each sample were reduced in DTT, carboxyamidomethylated, and digested with Porozyme immobilized trypsin at 37 °C overnight (Applied Biosystems, Foster City, CA, USA).[24] The digested samples were desalted using solid phase extraction with SPEC-PLUS PT C18 columns (Varian, Lake Forest, CA, USA).

Enrichment of phosphopeptides with gallium-immobilized metal affinity chromatography

The desalted peptides were vacuum-dried and reconstituted in 250 mM acetic acid in 30% acetonitrile (ACN) to a final volume of 50 μL. Gallium silica spin columns (55416-U, Sigma-Aldrich, St. Louis, MO, USA) were washed and equilibrated with 50 μL 250 mM acetic acid in 30% ACN. The samples were added to the equilibrated column and loaded by centrifugation for 30 s at 500 × *g*. The depleted flow-through liquid was reserved. The columns were incubated for 15 min at room temperature and then washed three times with 50 μL 250 mM acetic acid in 30% ACN. The flow-through liquid from the first wash was collected and combined with the previous reserve (∼100 μL total). The spin column was finally washed with 50 μL water. Phosphopeptides were eluted once with 25 μL 10% phosphoric acid and then 3 more times, and all 4 eluents were combined (∼100 μL total).

MudPIT

The enriched phosphopeptide fractions and the phosphopeptide-depleted, flow-through fractions were separately analyzed by liquid chromatography-tandem mass spectrometry, also known as MudPIT. The peptides were loaded off-line and then separated on-line on home-made biphasic columns prepared from 365 outer diameter × 75 μm inner diameter-fused silica with a 5-μm tip and packed with 9 cm of reverse phase C18 resin (Aqua, 5 μm, Phenomenex, Torrance, CA, USA) followed by 4 cm of strong cation exchange resin (Luna, 5 μm, Phenomenex). A 12-step elution procedure consisting of stepwise increasing concentrations of salt solution followed by increasing gradients of organic mobile phase was used.[24] Solvent flow was 200 nL min^{-1} and was controlled with an Accela HPLC pump (Thermo Fisher Scientific, Waltham, MA, USA) and a T-split junction where 2,100 V electricity was applied.[24] The eluent was electrosprayed directly into the orifice of an LTQ-Orbitrap XL mass spectrometer (Thermo Fisher Scientific) controlled by Xcalibur 2.0.7 software (Thermo Fisher Scientific). A parent-ion scan was performed in the Orbitrap over the range of 400–1600 m/z at 30 000 resolution, with 500 000 automatic gain control (AGC), 500 ms ion injection time, and 1 μscan. Lock-mass was enabled.[84] Data-dependent MS^2 and MS^3 were performed in the linear ion trap with 10 000 AGC and 100 ms ion injection times with 1 μscan. MS^2 was performed on the ten most intense MS ions, and MS^3 was triggered if one of the top three MS^2 ions corresponded with neutral loss of 98.0, 49.0, and 32.7 Da for +1, +2 and +3 charged ions, respectively.[69] Minimum signals were 1000 and 500 respectively. An isolation width of 2 m/z and normalized collision energy of 35% were used for MS^2 and MS^3. Dynamic exclusion was used with repeat count of 2, 30 s repeat duration, a list of 500, list duration of 2 min and exclusion mass width of ±0.7 Da. For the specific detection of peptides with known masses, the instrument parameters were the same except that dynamic exclusion was not enabled and specific masses were placed on a limited parent mass list in Xcalibur. The following peptides were evaluated [HIANLAGNPK, 517.79 m/z (+2); WYEIASFPSR, 628.31 m/z (+2), and KIVCDPSYLPNK, 717.89 m/z (+2)].

Mascot searching

MS^2 and MS^3 spectrum data files were separately extracted from the raw data with Bioworks 3.3.1 (Thermo Fisher Scientific) using the parameters 600–4500 mass range, 0 group scan, 1 minimum group count, and 5 minimum ion counts. For each sample, the MS^2 and MS^3 spectra collected for the depleted flow-through peptide fraction and the phosphopeptide-enriched fraction were pooled respectively. In addition, all of the MS^2 spectra collected from all 4 ET-treatments and AIR controls were pooled respectively (1 251 278 total spectra for AIR and 1 282 272 spectra for ET). The same was done for the MS^3 spectra (2528 and 4274 spectra respectively for AIR and ET). Spectral data sets were pooled to reduce random sampling effects associated with MudPIT and increase the statistical confidence associated with reproducible detection of proteins.[31,32] Sets of MS^2 and MS^3 spectra were searched with Mascot 2.3.0.[29] For MS^2 spectra, search parameters were for tryptic digests, 1 possible missed cleavage, fixed amino acid modification [+57, C], variable amino acid modifications [+18, M] and [+80, S, T], monoisotopic mass values, ±10 ppm parent ion mass tolerance, ±0.8 Da fragment ion mass tolerance, and #13C = 1 enabled. For MS^3 spectra, search parameters were for tryptic digests, 1 possible missed cleavage, fixed amino acid modification [+57, C], variable amino acid modifications [–18, S], [–18, T] [+18, M] and [+80, S, T] , monoisotopic mass values, ±1.5 Da parent ion mass tolerance, and ±0.8 Da fragment ion mass tolerance. The searched database consisted

of version 8.0 of the *A. thaliana* genome protein reference database (ftp://ftp.arabidopsis.org/home/tair/Sequences/blast_datasets/, 32 825 records) appended with a list of common contaminants (32 997 records total).

Protein identification

Mascot output was processed by a modified, 64-bit version of PANORAMICS[2], a probability-based program that determines the likelihood that peptides are correctly assigned to proteins.[30,31] PANORAMICS[2] first considers all peptide matches made by Mascot and calculates the probability that these matches are correct (analysis was limited to peptides having Mascot Ions score-Identity score differences not less than −5). Peptides also identified by corroborating MS^3 spectra received increased Ions scores if additional peptide-determining fragment ions were detected.[30] PANORAMICS[2] considered the probabilities for both distinct peptides and shared peptides in a coherent manner and distributed the probabilities of shared peptides among all related proteins. The Mascot Ions Score, the database size and the length and charge state of each peptide sequence are part of the probability model. The reported protein probability indicates that a parsimonious protein group was correctly identified by the matched peptides. A protein group can consist of one or more proteins identified by the same set of peptides. Protein groups were ultimately treated as single proteins with one record being arbitrarily chosen as the representative of the group. The probability that a protein identification was not correct (false-positive rate) is 1 minus the calculated protein probability and agrees with false-positive rates that can be deduced by reverse database searching.[30,85] Peptide sequence matches, Mascot scores, protein group probabilities and other relevant data are provided (Tables S1, S2, ESI).† The positions of amino acid modifications are indicated by the variable modification string (for MS^2, 0 = no modification, 1 = oxidized M, 2 = phosphorylated S or T; for MS^3, 0 = no modification, 1 = dehydrated S, 2 = dehydrated T, 3 = oxidized M and 4 = phosphorylated S or T). The amino acid positions of neutral loss are indicated by the neutral loss string (0 = position not modified so neutral loss not considered, 1 = neutral loss observed for the variable modification indicated, 2 = neutral loss not observed for the variable modification indicated).

Relative quantification of proteins

Because of random sampling effects associated with MudPIT,[31,32] it was difficult to determine if the absence of any protein/peptide was a result of a specific treatment or a by-product of the chance of not detecting it. Therefore, quantitative analysis was limited to proteins that were detected from the pooling of spectra from all 4 replicate experiments in both ET-treated and control seedlings. In addition, plant proteins having at least 1 spectral count in each of three treatments were kept if the probability for a given protein in at least one of the treatments exceeded the 0.95 probability threshold and exceeded 0.90 in the other. There were 3814 proteins that satisfied these requirements. A spectrum assigned to a peptide was counted if an Ion score produced a positive probability, which required the Mascot Ions score/Identity score difference to be not less than −10, and if the score was top-ranking. The score differential for counting is different than that for the probability model because counting lower-scoring spectra for higher-confidence peptides improves the accuracy of measuring different amounts of proteins between samples.[31] The count for a distinct peptide was based on the total number of spectra satisfying the preceding criteria while a count for a shared peptide was divided by the number of protein groups with which it was shared.[31] The numbers of spectra contributing to the identification of all shared and distinct peptides assigned to a protein group for each treatment were summed. A G-test was used to assess the statistical differences of the spectral counts per treatment,[36] with the hypothesis being that the spectral count of any protein A was equal across 2 treatments. The advantage of the G-test is that spectral datasets for replicates can be combined rather than treated separately. This reduces MS^2 random sampling errors by increasing the numbers of spectra associated with peptides, which in turn favors statistically reproducible protein identification.[31] Normalization values were the total sum of spectral counts for all considered proteins in each pooled set of data. The corresponding *p*-value was calculated from X^2 distribution with 1 degree of freedom. QVALUE software was used to estimate *q*-values [*i.e.* FDR; $q = 0.01$)] from *p*-values.[86] The records of the proteins found from the spectra combined from 4 experiments (or groups of proteins sharing the same set of observed peptides) with statistically different summed spectral counts are listed in Table S3 (ESI) along with Gene Ontology descriptions and whether the proteins have predicted transmembrane domains.†

Polyacrylamide gel electrophoresis and Western blotting

Fifty μg protein from microsomal membrane preparations were mixed with LDS sample buffer and separated on 4–12% Bis-Tris NuPAGE gels according to manufacturer instructions (Invitrogen, Carlsbad, CA, USA). Separated proteins were electrophoretically transferred onto a PVDF membrane (BIO-RAD, Hercules, CA, USA) using a Mini Trans-Blot Cell (BIO-RAD) according to instructions. To detect ECA1, a 1 : 3000 dilution of anti-ECA1 antibody [26] provided by Dr Heven Sze (University of Maryland, College Park, MD, USA) was used, followed by a 1 : 5000 dilution of goat anti-rabbit horseradish peroxidase secondary antibody (Pierce Protein Research Products, Thermo Fisher Scientific). Immuno-decorated proteins were visualized by enhanced chemiluminescence detection using the SuperSignal West Femto Maximum Sensitivity Substrate (Pierce Protein Research Products, Thermo Fisher Scientific). Images were captured with a CCD camera (Fuji LAS-3000, Fujifilm Corp., Tokyo, Japan).

High-resolution, time-lapse imaging

Seeds were sown on agar medium containing AVG, as before, kept for 2 days at 4° C and exposed to fluorescent light for 2 to 4 h. For growth response kinetics measurements, seedlings were treated for 1 h with ET-free air followed by 2 h with 1 μL/L ET. This was followed by 5 h ET-free air treatment to

allow for growth recovery. Time-lapse imaging of hypocotyls on vertically oriented plates was conducted as previously described[20–22] using a Marlin CCD camera (Allied Vision Technology, Newburyport, MA, USA) and infra-red illumination. Images were captured every 5 min for 8 h. Growth rate was determined as previously described.[21,22] Data were normalized to basal growth rate in ET-free air prior to treatment with ET. Experiments were repeated at least three separate times and at least four seedlings were measured. For nutational bending experiments, seedlings were treated with 1 μL/L ET for 24 h and the angles of hypocotyls were measured manually as previously described.[20] The nutational amplitude was determined by measuring the change in angle from the peak of each oscillation to the midline of the sine wave. For each seedling, the peak nutational amplitude was determined. Experiments were repeated at least 4 times and at least six seedlings examined.

Abbreviations

ACC	1-aminocyclopropane-1-carboxylic acid
AGC	automatic gain control
ACN	acetonitrile
AVG	1-aminoethoxyvinylglycine
BR	brassinosteroid
ER	endoplasmic reticulum
ET	ethylene
FDR	false discovery rate
GSH	glutathione
MudPIT	Multidimensional Protein Identification Technology
SAM	S-adenosylmethionine
TAIR	The Arabidopsis Information Resource
TF	transcription factor

Acknowledgements

We thank Jianhong Chang at the University of Maryland for early trials to test seed sowing procedures, ET treatments, and collecting seedlings in the dark. This work was supported in part by a grant from NSF (MCB0923796) to Dr Chang and a Specific Cooperative Agreement between the University of Maryland and USDA-ARS. Dr Chang is supported in part by the Maryland Agricultural Experiment Station.

References

1 F. Vandenbussche and D. Van Der Straeten, *J. Plant Growth Regul.*, 2007, **26**, 178–187.
2 C. H. Dong, M. Rivarola, J. S. Resnick, B. D. Maggin and C. Chang, *Plant J.*, 2008, **53**, 275–286.
3 C. Grefen, K. Stadele, K. Ruzicka, P. Obrdlik, K. Harter and J. Horak, *Mol. Plant*, 2008, **1**, 308–320.
4 B. P. Hall, S. N. Shakeel and G. E. Schaller, *J. Plant Growth Regul.*, 2007, **26**, 118–130.
5 Y. F. Chen, M. D. Randlett, J. L. Findell and G. E. Schaller, *J. Biol. Chem.*, 2002, **277**, 19861–19866.
6 Y. F. Chen, S. N. Shakeel, J. Bowers, X. C. Zhao, N. Etheridge and G. E. Schaller, *J. Biol. Chem.*, 2007, **282**, 24752–24758.
7 Z. Gao, C. K. Wen, B. M. Binder, Y. F. Chen, J. Chang, Y. H. Chiang, R. J. Kerris, 3rd, C. Chang and G. E. Schaller, *J. Biol. Chem.*, 2008, **283**, 23801–23810.
8 R. L. Gamble, X. Qu and G. E. Schaller, *Plant Physiol.*, 2002, **128**, 1428–1438.
9 W. Wang, A. E. Hall, R. O'Malley and A. B. Bleecker, *Proc. Natl. Acad. Sci. U. S. A.*, 2003, **100**, 352–357.
10 J. J. Kieber, M. Rothenberg, G. Roman, K. A. Feldmann and J. R. Ecker, *Cell*, 1993, **72**, 427–441.
11 P. B. Larsen and C. Chang, *Plant Physiol.*, 2001, **125**, 1061–1073.
12 S. D. Yoo, Y. H. Cho, G. Tena, Y. Xiong and J. Sheen, *Nature*, 2008, **451**, 789–795.
13 K. L. Clark, P. B. Larsen, X. Wang and C. Chang, *Proc. Natl. Acad. Sci. U. S. A.*, 1998, **95**, 5401–5406.
14 Z. Gao, Y. F. Chen, M. D. Randlett, X. C. Zhao, J. L. Findell, J. J. Kieber and G. E. Schaller, *J. Biol. Chem.*, 2003, **278**, 34725–34732.
15 J. M. Alonso, T. Hirayama, G. Roman, S. Nourizadeh and J. R. Ecker, *Science*, 1999, **284**, 2148–2152.
16 M. M. Bisson, A. Bleckmann, S. Allekotte and G. Groth, *Biochem. J.*, 2009, **424**, 1–6.
17 F. An, Q. Zhao, Y. Ji, W. Li, Z. Jiang, X. Yu, C. Zhang, Y. Han, W. He, Y. Liu, S. Zhang, J. R. Ecker and H. Guo, *Plant Cell*, 2010, **22**, 2384–2401.
18 P. Guzman and J. R. Ecker, *Plant Cell*, 1990, **2**, 513–523.
19 C. R. Darwin, *The Power of Movement in Plants*, John Murray, London, 1880.
20 B. M. Binder, R. C. O'Malley, W. Wang, T. C. Zutz and A. B. Bleecker, *Plant Physiol.*, 2006, **142**, 1690–1700.
21 B. M. Binder, C. O'Malley R, W. Wang, J. M. Moore, B. M. Parks, E. P. Spalding and A. B. Bleecker, *Plant Physiol.*, 2004, **136**, 2913–2920.
22 B. M. Binder, L. A. Mortimore, A. N. Stepanova, J. R. Ecker and A. B. Bleecker, *Plant Physiol.*, 2004, **136**, 2921–2927.
23 H. Qiao, K. N. Chang, J. Yazaki and J. R. Ecker, *Genes Dev.*, 2009, **23**, 512–521.
24 L. Florens and M. P. Washburn, *Methods Mol. Biol.*, 2006, **328**, 159–175.
25 P. Spanu, G. Felix and T. Boller, *Plant Physiol.*, 1990, **93**, 1482–1485.
26 F. Liang, K. W. Cunningham, J. F. Harper and H. Sze, *Proc. Natl. Acad. Sci. U. S. A.*, 1997, **94**, 8579–8584.
27 U. K. Aryal, D. J. Olson and A. R. Ross, *J. Biomol. Tech.*, 2008, **19**, 296–310.
28 A. Makarov, E. Denisov, A. Kholomeev, W. Balschun, O. Lange, K. Strupat and S. Horning, *Anal. Chem.*, 2006, **78**, 2113–2120.
29 D. N. Perkins, D. J. Pappin, D. M. Creasy and J. S. Cottrell, *Electrophoresis*, 1999, **20**, 3551–3567.
30 J. Feng, W. M. Garrett, D. Q. Naiman and B. Cooper, *J. Proteome Res.*, 2009, **8**, 5396–5405.
31 B. Cooper, J. Feng and W. M. Garrett, *J. Am. Soc. Mass Spectrom.*, 2010, **21**, 1534–1546.
32 H. Liu, R. G. Sadygov and J. R. Yates, 3rd, *Anal. Chem.*, 2004, **76**, 4193–4201.
33 G. E. Tusnady and I. Simon, *Bioinformatics*, 2001, **17**, 849–850.
34 L. Brechenmacher, J. Lee, S. Sachdev, Z. Song, T. H. Nguyen, T. Joshi, N. Oehrle, M. Libault, B. Mooney, D. Xu, B. Cooper and G. Stacey, *Plant Physiol.*, 2009, **149**, 670–682.
35 J. Lee, W. M. Garrett and B. Cooper, *J. Sep. Sci.*, 2007, **30**, 2225–2230.
36 B. Zhang, N. C. VerBerkmoes, M. A. Langston, E. Uberbacher, R. L. Hettich and N. F. Samatova, *J. Proteome Res.*, 2006, **5**, 2909–2918.
37 Y. Zhang, Z. Wen, M. P. Washburn and L. Florens, *Anal. Chem.*, 2009, **81**, 6317–6326.
38 Y. Zhang, Z. Wen, M. P. Washburn and L. Florens, *Anal. Chem.*, 2010, **82**, 2272–2281.
39 T. Z. Berardini, S. Mundodi, L. Reiser, E. Huala, M. Garcia-Hernandez, P. Zhang, L. A. Mueller, J. Yoon, A. Doyle, G. Lander, N. Moseyko, D. Yoo, I. Xu, B. Zoeckler, M. Montoya, N. Miller, D. Weems and S. Y. Rhee, *Plant Physiol.*, 2004, **135**, 745–755.
40 J. M. Alonso, A. N. Stepanova, T. J. Leisse, C. J. Kim, H. Chen, P. Shinn, D. K. Stevenson, J. Zimmerman, P. Barajas, R. Cheuk, C. Gadrinab, C. Heller, A. Jeske, E. Koesema, C. C. Meyers, H. Parker, L. Prednis, Y. Ansari, N. Choy, H. Deen, M. Geralt, N. Hazari, E. Hom, M. Karnes, C. Mulholland, R. Ndubaku, I. Schmidt, P. Guzman, L. Aguilar-Henonin, M. Schmid, D. Weigel, D. E. Carter, T. Marchand, E. Risseeuw, D. Brogden, A. Zeko, W. L. Crosby, C. C. Berry and J. R. Ecker, *Science*, 2003, **301**, 653–657.

41 W. Moeder, C. S. Barry, A. A. Tauriainen, C. Betz, J. Tuomainen, M. Utriainen, D. Grierson, H. Sandermann, C. Langebartels and J. Kangasjarvi, *Plant Physiol*., 2002, **130**, 1918–1926.
42 L. Petruzzelli, I. Coraggio and G. Leubner-Metzger, *Planta*, 2000, **211**, 144–149.
43 A. Avni, B. A. Bailey, A. K. Mattoo and J. D. Anderson, *Plant Physiol*., 1994, **106**, 1049–1055.
44 V. Raz and J. R. Ecker, *Development*, 1999, **126**, 3661–3668.
45 S. D. Kopczak, N. A. Haas, P. J. Hussey, C. D. Silflow and D. P. Snustad, *Plant Cell*, 1992, **4**, 539–547.
46 J. Azimzadeh, P. Nacry, A. Christodoulidou, S. Drevensek, C. Camilleri, N. Amiour, F. Parcy, M. Pastuglia and D. Bouchez, *Plant Cell*, 2008, **20**, 2146–2159.
47 A. Pay, K. Resch, H. Frohnmeyer, E. Fejes, F. Nagy and P. Nick, *Plant J*., 2002, **30**, 699–709.
48 A. R. Paredez, S. Persson, D. W. Ehrhardt and C. R. Somerville, *Plant Physiol*., 2008, **147**, 1723–1734.
49 V. Parisy, B. Poinssot, L. Owsianowski, A. Buchala, J. Glazebrook and F. Mauch, *Plant J*., 2007, **49**, 159–172.
50 S. Yoshida, M. Tamaoki, M. Ioki, D. Ogawa, Y. Sato, M. Aono, A. Kubo, S. Saji, H. Saji, S. Satoh and N. Nakajima, *Physiol. Plant*, 2009, **136**, 284–298.
51 S. Cao, Z. Chen, G. Liu, L. Jiang, H. Yuan, G. Ren, X. Bian, H. Jian and X. Ma, *Plant Physiol. Biochem*., 2009, **47**, 308–312.
52 M. Kanwischer, S. Porfirova, E. Bergmuller and P. Dormann, *Plant Physiol*., 2005, **137**, 713–723.
53 C. Faso, Y. N. Chen, K. Tamura, M. Held, S. Zemelis, L. Marti, R. Saravanan, E. Hummel, L. Kung, E. Miller, C. Hawes and F. Brandizzi, *Plant Cell*, 2009, **21**, 3655–3671.
54 J. Zouhar, E. Rojo and D. C. Bassham, *Plant Physiol*., 2009, **149**, 1668–1678.
55 A. A. Sanderfoot, S. U. Ahmed, D. Marty-Mazars, I. Rapoport, T. Kirchhausen, F. Marty and N. V. Raikhel, *Proc. Natl. Acad. Sci. USA*, 1998, **95**, 9920–9925.
56 S. Bonsegna, S. P. Slocombe, L. De Bellis and A. Baker, *Arch. Biochem. Biophys*., 2005, **443**, 74–81.
57 T. Orth, S. Reumann, X. Zhang, J. Fan, D. Wenzel, S. Quan and J. Hu, *Plant Cell*, 2007, **19**, 333–350.
58 X. C. Zhang and J. P. Hu, *Mol. Plant*, 2008, **1**, 1036–1047.
59 J. L. Nemhauser, F. Hong and J. Chory, *Cell*, 2006, **126**, 467–475.
60 L. De Grauwe, F. Vandenbussche, O. Tietz, K. Palme and D. Van Der Straeten, *Plant Cell Physiol*., 2005, **46**, 827–836.
61 Z. Deng, X. Zhang, W. Tang, J. A. Oses-Prieto, N. Suzuki, J. M. Gendron, H. Chen, S. Guan, R. J. Chalkley, T. K. Peterman, A. L. Burlingame and Z. Y. Wang, *Mol. Cell Proteomics*, 2007, **6**, 2058–2071.
62 W. Tang, Z. Deng, J. A. Oses-Prieto, N. Suzuki, S. Zhu, X. Zhang, A. L. Burlingame and Z. Y. Wang, *Mol. Cell Proteomics*, 2008, **7**, 728–738.
63 A. J. Nagano, Y. Fukao, M. Fujiwara, M. Nishimura and I. Hara-Nishimura, *Plant Cell Physiol*., 2008, **49**, 969–980.
64 L. Du and B. W. Poovaiah, *Nature*, 2005, **437**, 741–745.
65 Y. Ide, N. Nagasaki, R. Tomioka, M. Suito, T. Kamiya and M. Maeshima, *J. Exp. Bot*., 2007, **58**, 1173–1183.
66 M. J. Wubben, 2nd, S. R. Rodermel and T. J. Baum, *Plant J*., 2004, **40**, 712–724.
67 J. B. Charron, F. Ouellet, M. Houde and F. Sarhan, *BMC Plant Biol*., 2008, **8**, 86.
68 J. H. Kim, H. R. Woo, J. Kim, P. O. Lim, I. C. Lee, S. H. Choi, D. Hwang and H. G. Nam, *Science*, 2009, **323**, 1053–1057.
69 S. A. Beausoleil, M. Jedrychowski, D. Schwartz, J. E. Elias, J. Villen, J. Li, M. A. Cohn, L. C. Cantley and S. P. Gygi, *Proc. Natl. Acad. Sci. USA*, 2004, **101**, 12130–12135.
70 M. Aguiar, W. Haas, S. A. Beausoleil, J. Rush and S. P. Gygi, *J. Proteome Res*., 2010, **9**, 3103–3107.
71 A. M. Palumbo and G. E. Reid, *Anal. Chem*., 2008, **80**, 9735–9747.
72 B. Cooper, *J. Proteome Res*., 2011, **10**, 1432–1435.
73 A. Motchoulski and E. Liscum, *Science*, 1999, **286**, 961–964.
74 H. Harada, T. Kuromori, T. Hirayama, K. Shinozaki and R. A. Leigh, *J. Exp. Bot*., 2004, **55**, 2005–2014.
75 T. Ishida, Y. Kaneko, M. Iwano and T. Hashimoto, *Proc. Natl. Acad. Sci. USA*, 2007, **104**, 8544–8549.
76 Y. H. Shi, S. W. Zhu, X. Z. Mao, J. X. Feng, Y. M. Qin, L. Zhang, J. Cheng, L. P. Wei, Z. Y. Wang and Y. X. Zhu, *Plant Cell*, 2006, **18**, 651–664.
77 J. Cela, J. Falk and S. Munne-Bosch, *FEBS Lett*., 2009, **583**, 992–996.
78 A. De Paepe, M. Vuylsteke, P. Van Hummelen, M. Zabeau and D. Van Der Straeten, *Plant J*., 2004, **39**, 537–559.
79 S. Kepinski and O. Leyser, *Plant Cell*, 2002, **14**(Suppl), S81–95.
80 J. Smalle, J. Kurepa, P. Yang, E. Babiychuk, S. Kushnir, A. Durski and R. D. Vierstra, *Plant Cell*, 2002, **14**, 17–32.
81 J. Smalle, J. Kurepa, P. Yang, T. J. Emborg, E. Babiychuk, S. Kushnir and R. D. Vierstra, *Plant Cell*, 2003, **15**, 965–980.
82 S. Yanagisawa, S. D. Yoo and J. Sheen, *Nature*, 2003, **425**, 521–525.
83 W. E. Friedman, *Am. J. Bot*., 2009, **96**, 5–21.
84 J. V. Olsen, L. M. de Godoy, G. Li, B. Macek, P. Mortensen, R. Pesch, A. Makarov, O. Lange, S. Horning and M. Mann, *Mol. Cell Proteomics*, 2005, **4**, 2010–2021.
85 J. Feng, D. Q. Naimain and B. Cooper, *Anal. Chem*., 2007, **79**, 3901–3911.
86 J. D. Storey and R. Tibshirani, *Proc. Natl. Acad. Sci. USA*, 2003, **100**, 9440–9445.

